

Modulation of Blood Fluke Development in the Liver by Hepatic CD4⁺ Lymphocytes

Stephen J. Davies,¹ Jane L. Grogan,² Rebecca B. Blank,¹
K. C. Lim,¹ Richard M. Locksley,² James H. McKerrow^{1*}

We have identified an alternate developmental pathway in the life cycle of the trematode pathogen *Schistosoma mansoni*. This pathway is used in immunodeficient hosts in which the parasite fails to receive appropriate signals from the host immune system. Helminth development is altered at an early stage during infection, resulting in the appearance of attenuated forms that prolong survival of host and parasite. Hepatic CD4⁺ T lymphocyte populations are an integral component of the immune signal recognized by the parasite.

The relationship between schistosome (blood fluke) parasites and their human hosts is ancient and long-lived. Parasites can survive for decades within infected hosts, and unlike most bacteria, protists, and viruses, schistosomes and other helminths induce chronic infections where host and parasite survive for years, maximizing the parasite's opportunity for reproduction and transmission (1). For some helminths, there is evidence that host factors can trigger alternate developmental pathways that facilitate survival in the face of adverse conditions (2, 3). This phenomenon may contribute to the aggregated distribution of infection levels and morbidity observed in infected host populations (1).

Previous studies (4, 5) have suggested that a highly evolved relationship exists between schistosomes and their hosts that may include parasite exploitation of host endocrine and immune signals. To investigate the latter possibility further, we examined *S. mansoni* parasites isolated from recombination activating gene-1 deficient (RAG-1^{-/-}) C57BL/6 mice (6) that lack B and T lymphocytes (7). At day 26 post infection (p.i.), parasites from the livers of RAG-1^{-/-} mice were small, uniform in size, and undifferentiated (Fig. 1A), indicating they had not initiated the period of rapid growth characteristic of parasites isolated from wild-type mice at this time point. Schistosomes from RAG-1^{-/-} animals were still significantly smaller than those from wild-type mice at days 42 and 56 p.i. (Fig. 1A). A stunted developmental phenotype was also evident in *S. japonicum* worms isolated from RAG-2^{-/-} BALB/c mice (Fig. 1B), suggesting that this phenomenon is conserved

amongst the Schistosomatidae (8). Similar results were obtained with *S. mansoni* with the use of mice homozygous for the *Prkdc*^{scid} allele (9), which also lack functional B and T lymphocytes (10). Attenuated parasite development resulted in delayed sexual maturation, evidenced by reduced numbers of paired worms at day 35 and 42 p.i. (Fig. 1C). Attenuated development was not a secondary effect of delayed migration, because parasites arrived in the portal system of RAG-1^{-/-} mice with the same kinetics as in wild-type mice (9). Attenuated development during prepatency was accompanied by dramatically reduced accumulation of eggs in the liver

(Fig. 1D), attributable both to a delay in the onset of egg production and to reduced egg production (11). Eggs recovered from the livers of RAG-1^{-/-} mice were fully capable of hatching, and the resulting miracidia were infectious for *Biomphalaria glabrata* snails, indicating that the eggs produced were viable (9).

Our previous work identified a role for TNF in stimulating egg production by adult schistosomes (5). However, absence of TNF or TNF receptor (TNFR) signaling did not result in early developmental or egg-laying defects in *S. mansoni* (12), suggesting that TNF effects are exerted only on adult parasites. Likewise, deficiencies in other cytokines and key signaling molecules failed to perturb schistosome development (13).

Previous work showed that *S. mansoni* growth was impaired in IL-7^{-/-} mice and suggested that this was due to a direct interaction between IL-7 and the parasite (14). However, our data provide an alternative explanation for these results, considering the lymphopenic phenotype of IL-7^{-/-} mice (15). We have observed attenuated development in similarly lymphopenic IL-7R^{-/-} mice (9), which express IL-7 but do not respond to it (16).

To determine whether absence of a specific B or T lymphocyte population was responsible for modulating schistosome development, we examined *S. mansoni* infections in immunoglobulin heavy chain (Igh)6^{-/-}

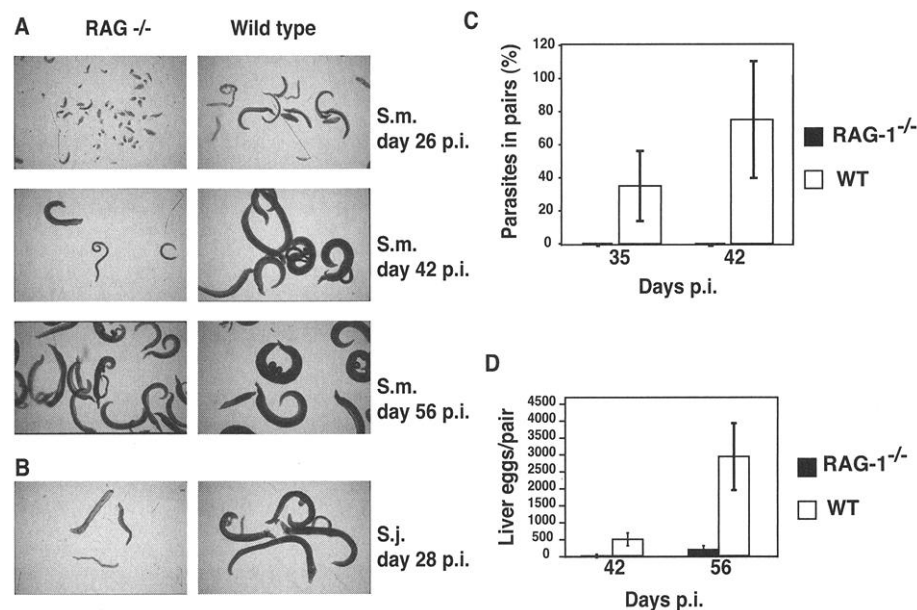


Fig. 1. Schistosome development in B cell- and T cell-deficient hosts. (A) *Schistosoma mansoni* isolated from RAG-1^{-/-} and wild-type C57BL/6 mice at the time points indicated p.i. (25× magnification). (B) *Schistosoma japonicum* isolated from RAG-2^{-/-} and wild-type BALB/c mice at day 28 p.i. (25× magnification). (C) Pairing of *S. mansoni* in RAG-1^{-/-} (black bars; value = 0) and wild-type mice (white bars) at days 35 and 42 p.i. were quantified as the percentage of total parasites participating in pairing. All values presented are averages ± SD, determined from groups of three to five animals. Results are representative of at least two individual experiments. (D) Egg production by *S. mansoni* in RAG-1^{-/-} (black bars) and wild-type C57BL/6 mice (white bars) at days 42 and 56 p.i.

¹Tropical Disease Research Unit, Department of Pathology, Veterans Affairs Medical Center, ²Howard Hughes Medical Institute, Department of Microbiology and Immunology, University of California San Francisco, CA 94143, USA.

*To whom correspondence should be addressed. E-mail: jmkc@cgl.ucsf.edu

REPORTS

mice that lack B cells (17), T cell receptor $\beta^{-/-}$ (TCR $\beta^{-/-}$) mice that lack $\alpha\beta$ T cells (18), TCR $\delta^{-/-}$ mice that lack $\gamma\delta$ T cells (19), and mice that are deficient in both TCR β and TCR δ (TCR $\beta^{-/-}$ /TCR $\delta^{-/-}$ mice) (20). As previously reported (21), parasite development was normal in Igh-6 $^{-/-}$ mice. However, in contrast to previous findings (22), we observed that *S. mansoni* development was impaired in TCR $\beta^{-/-}$ mice. Although there were no obvious differences in parasite size or pairing, early egg accumulation in the

liver—the most sensitive indicator of development during prepatency—was significantly lower in TCR $\beta^{-/-}$ mice, but not in TCR $\delta^{-/-}$ mice (Fig. 2A). Therefore, $\alpha\beta$ T cells but not $\gamma\delta$ T cells appear to modulate early schistosome development.

To further characterize the lymphocytes responsible for modulating parasite development, we reconstituted RAG-1 $^{-/-}$ mice with CD4 $^{+}$ or CD8 $^{+}$ T cells, or with CD19 $^{+}$ B cells, purified from wild-type C57BL/6 mice (23). Reconstitution with CD4 $^{+}$ cells rescued

schistosome development during prepatency, resulting in larger parasites, higher levels of pairing, and dramatically increased levels of egg production (Fig. 2B). Occasional increases in egg production were observed in CD8 $^{+}$ - and CD19 $^{+}$ -reconstituted RAG-1 $^{-/-}$ mice, but analysis of peripheral lymphocyte populations at necropsy revealed that all these animals contained significant numbers of CD4 $^{+}$ cells, expanded from contaminating CD4 $^{+}$ precursors (<1%). A positive correlation was observed between parasite egg production and numbers of reconstituting CD4 $^{+}$ lymphocytes (Fig. 2B) but not between egg production and CD8 $^{+}$ or CD19 $^{+}$ lymphocytes (Fig. 2B). To confirm the role of CD4 $^{+}$ lymphocytes in parasite development, we depleted CD4 $^{+}$ cells from wild-type mice in vivo by administering antibodies to CD4 (24). CD4 $^{+}$ lymphocyte depletion reduced egg production (Fig. 2C) to levels observed in TCR $\beta^{-/-}$ and TCR $\beta^{-/-}$ /TCR $\delta^{-/-}$ mice (Fig. 2A). Depletion of CD8 $^{+}$ cells (Fig. 2C) or $\gamma\delta$ T cells did not affect egg production (9). Therefore, CD4 $^{+}$ T lymphocytes were responsible for promoting early schistosome development.

In mammalian hosts, schistosome growth and development is initiated when parasites reach the liver, between 1 and 2 weeks p.i. (25). At 3 weeks p.i., developing parasites in the liver can be found in close association with perivascular accumulations of lymphoid cells that include CD4 $^{+}$ cells (26). We reasoned that CD4 $^{+}$ lymphocytes that populate the liver were the most likely candidates for the observed effects on schistosome development. In contrast to the spleen, where over 90% of CD4 $^{+}$ lymphocytes are major histocompatibility complex II (MHC II)-restricted

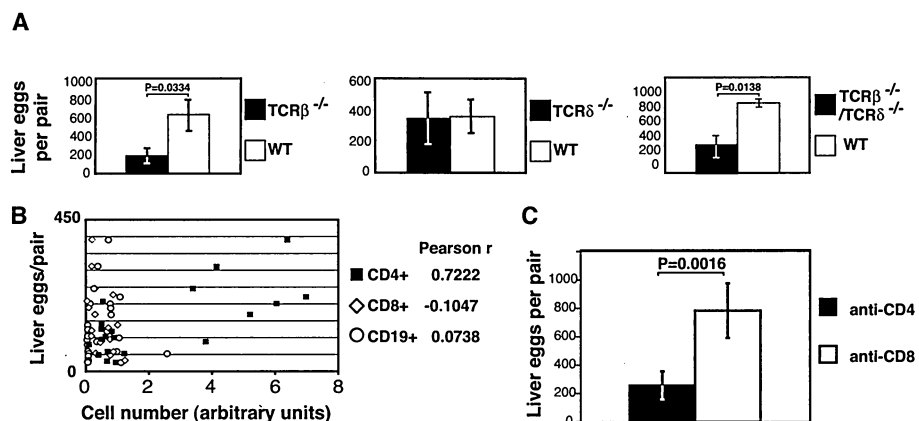


Fig. 2. The cells required for normal *S. mansoni* development are TCR $\alpha\beta^{+}$ and CD4 $^{+}$. (A) Egg production by *S. mansoni* in TCR $\beta^{-/-}$ (left), TCR $\delta^{-/-}$ (center), and TCR $\beta^{-/-}$ /TCR $\delta^{-/-}$ (right) C57BL/6 mice at day 42 p.i. All probability values (*P*) were calculated using *t* tests. (B) Relation between egg production and numbers of donor CD4 $^{+}$, CD8 $^{+}$, or CD19 $^{+}$ cells in RAG-1 $^{-/-}$ mice reconstituted with wild-type C57BL/6 lymphocytes. For each reconstituted animal, parasite egg production was plotted against the number of CD4 $^{+}$ (black squares), CD8 $^{+}$ (white diamonds), and CD19 $^{+}$ (white circles) cells present in the spleen. An estimate of absolute cell numbers (in arbitrary units) for each animal was calculated by multiplying the percentage of CD4 $^{+}$, CD8 $^{+}$, or CD19 $^{+}$ cells by the splenic mass. Correlation coefficients (Pearson *r*) between numbers of eggs and each cell type were calculated for each animal using Prism 3.02 software (GraphPad Software Inc., San Diego, California). Results are representative of three independent experiments. (C) Effect of in vivo depletion of CD4 $^{+}$ (black bar) or CD8 $^{+}$ (white bar) cells on *S. mansoni* egg production in wild-type C57BL/6 mice.

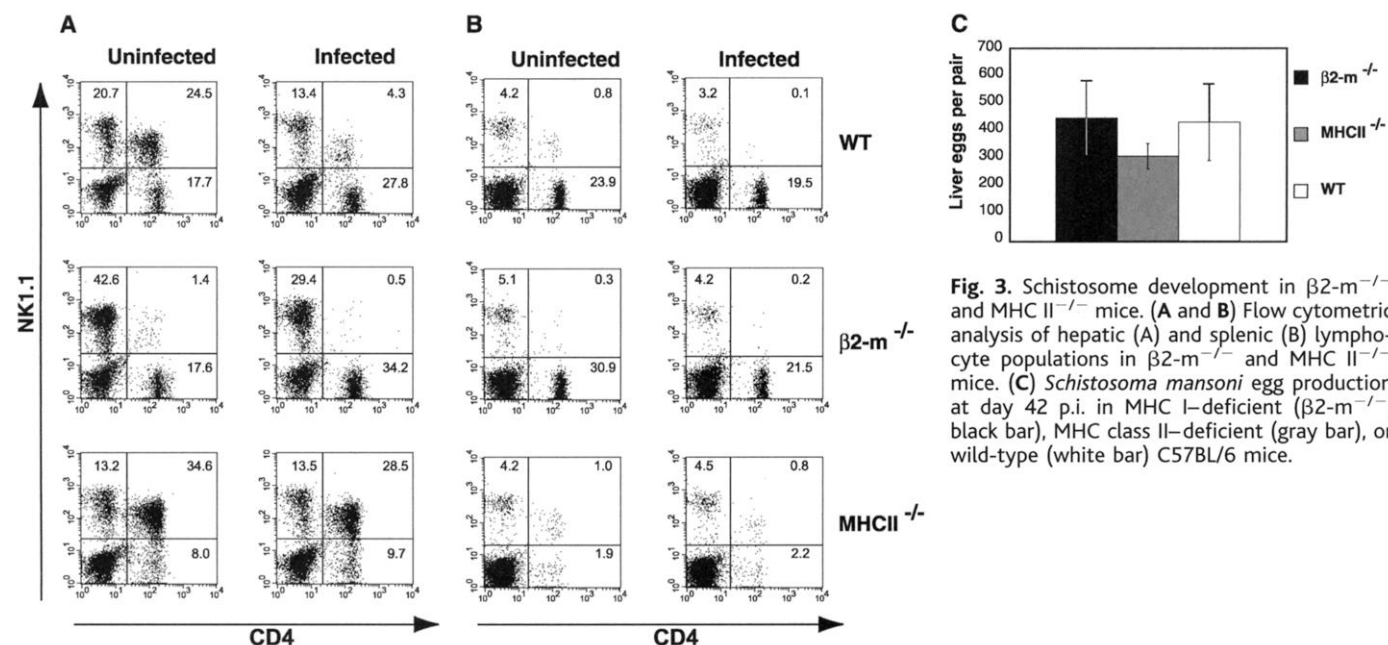


Fig. 3. Schistosome development in $\beta 2\text{-m}^{-/-}$ and MHC II $^{-/-}$ mice. (A and B) Flow cytometric analysis of hepatic (A) and splenic (B) lymphocyte populations in $\beta 2\text{-m}^{-/-}$ and MHC II $^{-/-}$ mice. (C) *Schistosoma mansoni* egg production at day 42 p.i. in MHC I-deficient ($\beta 2\text{-m}^{-/-}$, black bar), MHC class II-deficient (MHCII $^{-/-}$, gray bar), or wild-type (white bar) C57BL/6 mice.

REPORTS

T helper (T_H) cells (Fig. 3B), the hepatic $CD4^+$ compartment contains two major sub-populations (Fig. 3A) [(27), and references therein]: $CD4^+NK1.1^- T_H$ cells and $CD1d$ -restricted $CD4^+NK1.1^+$ natural killer T (NKT) cells. To determine which population was involved in schistosome development, we infected $\beta 2$ -microglobulin ($\beta 2$ -m) $^{-/-}$ mice that fail to express $CD1d$ and therefore lack $CD4^+$ NKT cells (Fig. 3A) (28), and MHC II $^{-/-}$ mice that lack $CD4^+$ T_H cells (Fig. 3, A and B) (29, 30). No schistosome developmental defects were observed in either $\beta 2$ -m $^{-/-}$ or MHC II $^{-/-}$ animals (Fig. 3C), indicating that either functional redundancy exists between $CD4^+$ T_H and NKT cells with respect to parasite development or another population of $CD4^+$ cells is involved which is neither $\beta 2$ -m- nor MHC II-dependent. In support of the latter possibility, we found that a sizable number of $CD4^+NK1.1^-$

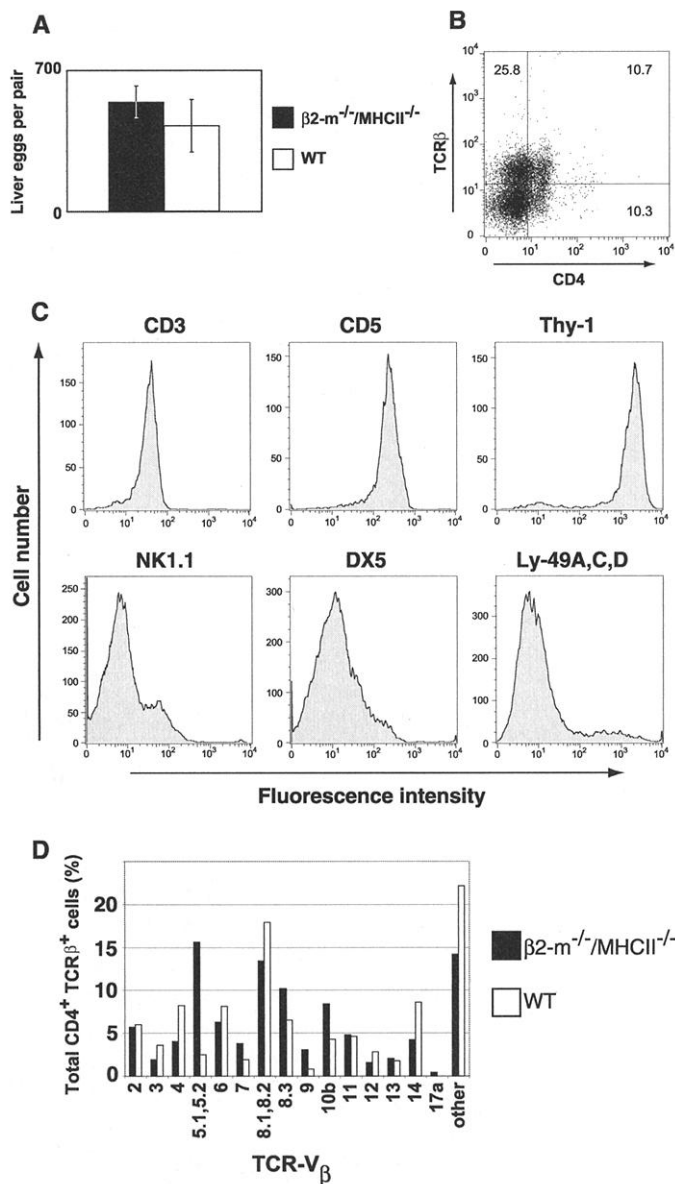
cells remained in the livers of MHC II $^{-/-}$ mice (Fig. 3A). These cells were absent from the spleens of MHC class II $^{-/-}$ mice (Fig. 3B) and therefore appeared to be specific to the liver.

To discriminate between the two possibilities, we infected mice that are deficient in both $\beta 2$ -m and MHC II ($\beta 2$ -m $^{-/-}$ /MHC II $^{-/-}$ mice) and therefore lack both $CD4^+$ T_H and NKT populations. Normal parasite development was observed in $\beta 2$ -m $^{-/-}$ /MHC II $^{-/-}$ mice (Fig. 4A), eliminating the possibility that functional redundancy occurs between hepatic $CD4^+$ T_H and NKT cells, and indicating that a third population of $CD4^+$ cells, one which is neither $\beta 2$ -m- nor MHC II-dependent, is involved in signaling normal parasite development. Examination of hepatic lymphocytes from $\beta 2$ -m $^{-/-}$ /MHC II $^{-/-}$ mice revealed a population of T lymphocytes with the predicted properties of both $CD4$ and

TCR β expression (Fig. 4B). These cells were not detected in the spleens of $\beta 2$ -m $^{-/-}$ /MHC II $^{-/-}$ mice, but comprised over 10% of the lymphocyte gate in the liver (Fig. 4B). The lymphoid morphology of these cells was confirmed by microscopic analysis (26). This population uniformly expressed molecules typically found on T lymphocyte populations, such as $CD3$, $CD5$, and $Thy-1$ (Fig. 4C), but the majority did not express the NK/NKT cell markers $NK1.1$, $DX5$, and $Ly-49A/C/D$ (Fig. 4C) (31). To further examine the similarity between this $CD4^+$ TCR β^+ T lymphocyte population and NKT cells, we analyzed their TCR V_β repertoire (32), because NKT cells are distinctive in their expression of predominantly $V_\beta 2$, -7, and -8. Unlike NKT cells, we found that $CD4^+$ TCR β^+ T lymphocytes from the livers of $\beta 2$ -m $^{-/-}$ /MHC II $^{-/-}$ mice express a diverse V_β repertoire (Fig. 4D); all V_β chains analyzed were detectable at significant levels except for $V_\beta 17a$, which is not expressed by mice with the C57BL genetic background. In most respects, the V_β repertoire closely resembles that of peripheral $CD4^+$ TCR β^+ T cells from wild-type C57BL/6 mice (Fig. 4D), with the exception of a sixfold increase in $V_\beta 5.1$ or -5.2 expression in hepatic $CD4^+$ TCR β^+ T lymphocytes from $\beta 2$ -m $^{-/-}$ /MHC II $^{-/-}$ mice (Fig. 4D). We conclude that this previously unrecognized population of $CD4^+$ TCR β^+ T cells, that is liver-specific in distribution and independent of both $\beta 2$ -m and MHC II, participates in signaling for normal schistosome development in the livers of $\beta 2$ -m $^{-/-}$ /MHC II $^{-/-}$ mice.

We have identified an alternative developmental program in the life cycle of a trematode pathogen that allows the parasite to modulate development in response to a host immune signal. In the absence of this signal, this developmental pathway is initiated, possibly to allow worm development to "arrest," and the host to survive, until optimal conditions for growth and transmission return. A mechanism that permits the parasite to adjust to differences in host immunocompetence has obvious selective advantages, particularly in heterogeneous host populations that exhibit great variation in immunocompetence and in the presence of concomitant infections that may compromise the host's ability to sustain a helminth infection. Our findings may partly explain the observations of Karanja *et al.* (33) who reported decreased fecal egg outputs in patients with both *S. mansoni* and human immunodeficiency virus (HIV) infections. Our data show that an unusual population of lymphocytes with tissue specificity similar to that of the developing helminth can influence parasite development. Our results challenge current understanding of immune system organization and function within the liver, and they have important implications for under-

Fig. 4. Normal schistosome development in $\beta 2$ -m $^{-/-}$ /MHC II $^{-/-}$ mice reveals the presence of an unusual $CD4^+$ TCR β^+ lymphocyte population in the liver. (A) Liver egg burdens at day 42 p.i. in $\beta 2$ -m $^{-/-}$ /MHC II $^{-/-}$ mice. (B) Flow cytometric analysis of $CD4$ and TCR β expression by hepatic lymphocytes from $\beta 2$ -m $^{-/-}$ /MHC II $^{-/-}$ mice. (C) Flow cytometric analysis of cell surface marker expression by hepatic $CD4^+$ TCR β^+ lymphocytes from $\beta 2$ -m $^{-/-}$ /MHC II $^{-/-}$ mice. (D) TCR V_β repertoire of hepatic $CD4^+$ TCR β^+ lymphocytes from $\beta 2$ -m $^{-/-}$ /MHC II $^{-/-}$ mice compared with the V_β repertoire of peripheral $CD4^+$ TCR β^+ lymphocytes from wild-type C57BL/6 mice.



standing modulation of helminth development in other host-parasite systems.

References and Notes

1. R. M. Maizels, D. A. Bundy, M. E. Selkirk, D. F. Smith, R. M. Anderson, *Nature* **365**, 797 (1993).
2. S. C. Harvey, A. W. Gemmill, A. F. Read, M. E. Viney, *Proc. R. Soc. Biol. Sci. Ser. B* **267**, 2057 (2000).
3. B. Ravindran, *Trends Parasitol.* **17**, 70 (2001).
4. R. A. Harrison, M. J. Doenhoff, *Parasitology* **86**, 429 (1983).
5. P. Amiri *et al.*, *Nature* **356**, 604 (1992).
6. Puerto Rican strain *S. mansoni* were maintained in the laboratory with the use of Syrian golden hamsters and *Biomphalaria glabrata* snails as hosts. RAG-1^{-/-} mice were purchased from Jackson Laboratory (Bar Harbor, ME). C57BL/6 mice were purchased from Charles River (Wilmington, MA). All animals were housed at the San Francisco Veteran Affairs Medical Center in accordance with protocols approved by the Institutional Animal Care and Use Committee. Mice were infected by exposure of the tail skin to 100 to 150 cercariae. Parasites were recovered from the portal system at various time points p.i. by perfusion, immediately fixed in 4% buffered formaldehyde, and photographed using a Nikon Microphot (Melville, NY) microscope at 25× magnification.
7. P. Mombaerts *et al.*, *Cell* **68**, 869 (1992).
8. *Oncomelania hupensis* infected with *S. japonicum* were obtained from F. A. Lewis (Biomedical Research Institute, Rockville, MD). RAG-2^{-/-} and wild-type BALB/c mice were purchased from Taconic (Germantown, NY).
9. S. J. Davies *et al.*, unpublished data.
10. K. Dorshkind *et al.*, *J. Immunol.* **132**, 1804 (1984).
11. To determine liver egg burdens, ~100 mg of liver tissue from the margin of the left lobe was digested in 0.7% trypsin (50 ml) in phosphate-buffered saline (PBS) for 1 hour at 37°C, and eggs were counted under a dissecting microscope.
12. No developmental or egg-laying defects were observed in TNF^{-/-}, TNF^{-/-}/lymphotoxin (LT)-α^{-/-}, or TNFR1^{-/-}/TNFR2^{-/-} mice (9), indicating that parasite development was not dependent on these cytokines or downstream effects of TNFR signaling.
13. Normal parasite development was observed in interferon (IFN)-γ^{-/-} mice (S. J. Davies, K. C. Lim, J. H. McKerrow, unpublished data), interleukin (IL)-4^{-/-} and IL-5^{-/-} mice (L. Rosa-Brunet, personal communication), and in signal transducer and activator of transcription (STAT)-4^{-/-} and STAT-6^{-/-} mice (R. B. Blank, K. C. Lim, S. J. Davies, J. H. McKerrow, unpublished data).
14. I. Wolowczuk *et al.*, *Infect. Immun.* **67**, 4183 (1999).
15. U. von Freeden-Jeffrey *et al.*, *J. Exp. Med.* **181**, 1519 (1995).
16. J. J. Peschon *et al.*, *J. Exp. Med.* **180**, 1955 (1994).
17. D. Kitamura, J. Roes, R. Kuhn, K. Rajewsky, *Nature* **350**, 423 (1991).
18. P. Mombaerts *et al.*, *Nature* **360**, 225 (1992).
19. S. Itohara *et al.*, *Cell* **72**, 337 (1993).
20. Igh-6^{-/-}, TCRβ^{-/-}, TCRδ^{-/-}, and TCRβ^{-/-}/TCRδ^{-/-} mice were purchased from Jackson Laboratory.
21. D. Jankovic *et al.*, *J. Exp. Med.* **187**, 619 (1998).
22. J. Iacomini, D. E. Ricklan, M. J. Stadecker, *Eur. J. Immunol.* **25**, 884 (1995).
23. For reconstitution experiments, lymph nodes from wild type C57BL/6 mice were dispersed through a 70-μm nylon strainer and cells were labeled with fluorescein isothiocyanate (FITC)-conjugated antibodies to CD8 and phycoerythrin (PE)-conjugated antibodies to CD19 (BD Pharmingen, San Diego, CA), and Alexa-conjugated antibodies to CD4 (Molecular Probes, Eugene, OR). CD8⁺, CD19⁺, or CD4⁺ cells were sorted to >99% purity after gating small, resting cells using forward- and side-scatter parameters (MoFlo Multi-Laser Flow Cytometer; Cytomation, Fort Collins, CO). 4 × 10⁶ cells were transferred into RAG-1^{-/-} mice by intravenous injection. Control mice received PBS alone. At necropsy, splenocytes from reconstituted RAG-1^{-/-} mice were surface labeled with tricolor (TC)-conjugated antibodies to CD4 (Santa Cruz Biotechnologies, Santa Cruz, CA),

- FITC-conjugated antibodies to CD8, and PE-conjugated antibodies to CD19 and analyzed using a FACScan flow cytometer with CellQuest software (Becton Dickinson, Franklin Lakes, NJ).
24. Antibodies used for depletion experiments were: GK1.5 (antibody to CD4; ATCC TIB-207); 3.155 (antibody to CD8; ATCC TIB-211); GL-3 (antibody to TCRγδ). Antibodies were purified by affinity chromatography and administered by intraperitoneal injection twice weekly at a dose of 1 mg per animal, beginning 1 week before infection and continuing until necropsy.
25. J. A. Clegg, *Exp. Parasitol.* **16**, 133 (1965).
26. Supplementary material is available at Science Online at www.sciencemag.org/cgi/content/full/294/5545/1358/DC1.
27. T. Abo, T. Kawamura, H. Watanabe, *Immunol. Rev.* **174**, 135 (2000).
28. M. Zijlstra *et al.*, *Nature* **344**, 742 (1990).
29. M. J. Grusby, R. S. Johnson, V. E. Papaioannou, L. H. Glimcher, *Science* **253**, 1417 (1991).
30. β2-m^{-/-} and MHC II^{-/-} mice were purchased from Jackson Laboratory and Taconic, respectively. At necropsy, livers were dispersed into single cell suspensions like spleens, but a 30% percoll gradient was used to separate hepatocytes from hepatic leukocytes before staining for cell surface molecules. Organs from at least three animals of each genotype and infection state were pooled for analysis. Cells were stained in the presence of unlabeled monoclonal antibodies to CD16 and CD32 ("Fc Block"; BD Pharmingen). Analysis was performed on a FACScan flow cytometer using CellQuest.
31. Flow cytometric analyses were performed using a MoFlo Multi-Laser Flow Cytometer, Alexa350-conjugated antibodies to CD4, allophycocyanin (APC)-conjugated antibodies to TCRβ, and the following additional antibodies, all in the presence of "Fc Block": FITC-conjugated antibodies to CD3 or antibodies to DX5, PE-conjugated antibodies to Thy-1 or antibodies to Ly-49A/C/D, and TC-conjugated CD5 or NK1.1.
32. For V_β analysis, cells were stained with CyChrome-conjugated antibodies to CD4, PE-conjugated antibodies to CD11b, and FITC-conjugated antibodies to V_β in the presence of "Fc Block." Binding of antibody to V_β binding was determined on the CD4⁺ CD11b⁻ population. Percentages were calculated by comparison with binding by a pan-TCRβ-specific antibody. Antibodies to V_β>17a were included as a negative control, because C57BL animals do not express V_β>17a.
33. D. M. Karanja, D. G. Colley, B. L. Nahlen, J. H. Ouma, W. E. Secor, *Am. J. Trop. Med. Hyg.* **56**, 515 (1997).
34. We thank C. Franklin and C. McArthur for technical assistance; K. A. Feldman for assistance with statistical analyses; L. Rosa-Brunet for communicating unpublished data; J. D. Sedgwick for TNF^{-/-} and TNF^{-/-}/LT^{-/-} mice; G. Yap for TNFR1^{-/-}/TNFR2^{-/-} mice; L. Lefrancois for the GL-3 anti-γδTCR hybridoma; and L. Rosa-Brunet, C. R. Caffrey, J. P. Salter, G. Grünig, K. Shinkai, J. C. Ryan, M. Dawes, L. L. Lanier, and J. A. Glaven for helpful discussions and advice. Microscopy was performed at the UCSF Liver Center Microscopy Core. Supported by National Institutes of Health grant AI10424 (to S.J.D.) and the Sandler Family Foundation (to J.H.M.).

17 July 2001; accepted 20 September 2001

Defective Antigen Processing in GILT-Free Mice

Maja Maric,¹ Balasubramanian Arunachalam,^{1*} Uyen T. Phan,¹ Chen Dong,^{1†} Wendy S. Garrett,¹ Kurt S. Cannon,¹ Christopher Alfonso,^{2‡} Lars Karlsson,² Richard A. Flavell,¹ Peter Cresswell^{1§}

Processing of proteins for major histocompatibility complex (MHC) class II-restricted presentation to CD4-positive T lymphocytes occurs after they are internalized by antigen-presenting cells (APCs). Antigenic proteins frequently contain disulfide bonds, and their reduction in the endocytic pathway facilitates processing. In humans, a gamma interferon-inducible lysosomal thiol reductase (GILT) is constitutively present in late endocytic compartments of APCs. Here, we identified the mouse homolog of GILT and generated a GILT knockout mouse. GILT facilitated the processing and presentation to antigen-specific T cells of protein antigens containing disulfide bonds. The response to hen egg lysozyme, a model antigen with a compact structure containing four disulfide bonds, was examined in detail.

Exposure of proteins internalized by APCs to the increasingly acidic and proteolytic environment of the endocytic pathway generates peptides that bind to MHC class II αβ dimers. The reduction of inter- or intrachain disulfide bonds, which facilitates this process, occurs within the endocytic pathway (1–5). To determine whether GILT, defined in humans (6), is involved in these reduction events, we elected to generate a knockout mouse. A search of the dbEST database from GenBank uncovered partial cDNAs encoding mouse GILT. By means of a 5' end RACE (rapid amplification of cDNA ends) polymerase chain reaction, we confirmed the sequence

and cloned the complete cDNA (GenBank accession number AF309649). Mouse GILT has about 70% amino acid sequence identity to human GILT, and the cysteine residues, including those in the active site (6), are highly conserved (Fig. 1A). A rabbit antiserum to mouse GILT was used to determine the intracellular localization of mouse GILT by immunofluorescence microscopy (7). GILT was colocalized with MHC class II and the lysosomal marker Lamp-2 in mouse dendritic cells (Fig. 2A); this pattern is similar to the distribution of GILT in human APCs.

Human GILT has both NH₂- and COOH-terminal peptides, which are removed in the